Hindawi
International Journal of Antennas and Propagation
Volume 2023, Article ID 7101049, 14 pages
https://doi.org/10.1155/2023/7101049

Research Article

A Car Logo Design-Inspired CPW-Fed Semitransparent Antenna for Vehicular Applications

Lekha Kannappan,[1] **Sandeep Kumar Palaniswamy**,[1] **Malathi Kanagasabai**,[2] **and Sachin Kumar**[1]

[1]*Department of Electronics and Communication Engineering, SRM Institute of Science and Technology, Kattankulathur, India*
[2]*Department of Electronics and Communication Engineering, College of Engineering, Anna University, Chennai, India*

Correspondence should be addressed to Sandeep Kumar Palaniswamy; vrpchs@gmail.com

Received 16 September 2022; Revised 8 October 2022; Accepted 18 May 2023; Published 27 May 2023

Academic Editor: Paolo Burghignoli

In this paper, a quad-port multiple-input multiple-output (MIMO) semitransparent antenna is designed for automotive applications. The transparent soda lime glass substrate is used in the prototype antenna for windshield applications, and the radiator is nontransparent copper metal. The unit cell radiator of the MIMO antenna is similar to the "NISSAN automobile-like" logo. The proposed MIMO antenna has a −10 dB impedance bandwidth of 3.4 to 11 GHz. The edge-to-edge distance between the elements in the MIMO configuration is 6 mm. The antenna elements are perpendicularly oriented to offer dual (horizontal and vertical) polarization, which aids in providing better isolation and good signal reception in all directions. The isolation between the resonating elements is greater than 15 dB without the use of any decoupling structure. The diversity metrics are examined in order to gain a better understanding of the MIMO antenna performance. The envelope correlation coefficient (ECC) is less than 0.01, diversity gain (DG) is greater than 9.98 dB, and the total active reflection coefficient (TARC) and channel capacity loss (CCL) are less than −10 dB and 0.07 bits/s/Hz, respectively. The quad-port MIMO antenna offers transparency of 52.26% over the entire area. The proposed antenna could be suitable for automotive applications such as intelligent transportation systems (ITS), vehicular communications, and the automatic vehicle identifier (AVI).

1. Introduction

With advancements in wireless technologies, various technological equipment have been introduced in the field of automotive electronics [1]. The new features meet additional infotainment and security requirements in the vehicle. The purpose of contemporary services is to ensure the comfort and safety of the driver [2]. Smart automobiles use a variety of wireless services, including GPS, GSM, Bluetooth, WLAN, and LTE, to function consistently. However, the number of antennas increases with the number of services in the vehicle [3]. The automotive antenna should be low-profile and occupy little space in the vehicle, and it should be placed far from the ground plane to compensate the ground losses. Also, the antenna placement should not affect the appearance of the vehicle. This necessitates the development of a multifunctional antenna. The low-profile antenna can be placed inside the shark-fin module to fit the vehicle's aerial configuration [4]. The prototype can also be placed in the side mirror cavity, chassis cavity, trunk, and bumper. For vehicular applications, multiband/broadband antennas are receiving a lot of attention from the researchers [5, 6].

Ultra-wideband (UWB) technology is widely used in a variety of applications, including automotive [7]. The electromagnetic coupling that occurs between the antenna elements in a MIMO system is referred as mutual coupling. When adjacent antenna elements have the same direction of current flow, mutual coupling increases. The spacing between the antenna elements must be considered for changing the interelement coupling. When there is inadequate space between the radiators, mutual coupling increases, resulting in deterioration of the radiation pattern

and impedance characteristics [8]. In the literature, mutual coupling has been addressed using electromagnetic band gap (EBG), decoupling networks, the frequency selective surface (FSS), the neutralization line, the defected ground structure (DGS), and isolation walls [9]. However, these structures complicate the antenna design. The isolation can also be increased by positioning the antenna elements orthogonally and increasing the space between them [10].

In [11], a UWB multiple-input multiple-output (MIMO) antenna with octagonal-shaped radiating elements was presented, with the elements positioned perpendicular to each other and the ground planes connected. In [12], a compact UWB MIMO antenna was designed for X-band, WLAN, and Wi-MAX frequencies. A four-element UWB MIMO antenna with isolation greater than 18 dB was presented in [13]. However, a transparent broadband or multiband antenna is required to easily install and save space in the vehicle without compromising its aesthetic appearance. In [14], a polyimide substrate-based transparent antenna with coplanar waveguide (CPW) feed was proposed to achieve wideband characteristics. A CPW-fed transparent antenna with indium tin oxide as the radiator was presented in [15]. In [16, 17], a tapered CPW-fed MIMO antenna with orthogonal elements and clove-shaped radiator was proposed for super-wideband characteristics, respectively. In [18], a semitransparent antenna was designed to operate in the ISM band, and its compactness and flexibility make it suitable for installation in a vehicle. A CPW-fed transparent antenna for WLAN and sub-6 GHz applications was developed in [19]. In [20], a transparent wideband antenna for 5G communication was designed on the plexiglass substrate, and rectangular branches were used to achieve wideband characteristics. In [21], canopy mesh was used for the radiator and the ground plane of the transparent antenna. In [22], a transparent glass was used as the substrate, and the antenna was suitable for 5G communications. In [23], a semitransparent antenna with a defected ground structure for increasing impedance was reported. In [24], a circular-shaped transparent monopole antenna was presented, and its conformability and flexibility make it suitable for vehicular communications. A transparent car logo design-inspired antenna was reported in [25], and when placed in the location of the brand logo, it has no effect on the appearance of the automobile.

In this work, a wideband UWB antenna is designed on the semitransparent substrate material. The proposed antenna is designed to be mounted on the windshield. The antenna radiator is a "NISSAN automobile-like" design, which does not affect the appearance of the vehicle. The ground plane is rectangular in shape, and a CPW feed is used to provide easy integration and a wide impedance bandwidth. The unit cell antenna is used to develop a four-port MIMO antenna configuration, and the diversity characteristics are studied. The diversity metrics are found to be within a practical range. The antenna housing results are also studied and found to be satisfactory for vehicular applications.

2. Antenna Design

Figure 1 depicts the layout and the fabricated prototype of the proposed antenna. The antenna is designed on the semitransparent soda lime glass (dielectric constant = 7.3) substrate of thickness of 1.1 mm, and copper is used for the ground plane and the radiator. The antenna radiator is similar to the "NISSAN automobile-like" logo, comprised of a circular ring with an inner radius of 6.3 mm, an outer radius of 8.5 mm, and a rectangular patch of 18 mm in the centre. The antenna design simulations are performed using the CST Microwave Studio tool [26].

In the proposed antenna design, finite ground coplanar waveguide feed is proposed. A conductor strip is used in the centre of a coplanar waveguide feed (CPW), which also has two ground planes on either side [27–29]. CPW feed is used for antenna feeding due to its low dispersion, broadband performance, and ease of implementation. The length and width of the ground plane are 7 mm and 11.2 mm, respectively. The proposed antenna prototype has a total footprint of 25 mm × 25 mm. The impedance bandwidth of the antenna ranges from 3.4 to 11 GHz. Figure 2 depicts the evolution stages and reflection coefficients of the proposed unit cell. The antenna design starts with a CPW-fed circular monopole radiator (evolution 1) and a modified ground plane that covers a wide bandwidth range. The circular patch is then evolved into a circular ring (evolution 2), with a rectangular stub added in the middle of it (evolution 3). Evolution 2 and evolution 3 are proposed to achieve the desired shape of NISSAN automobile logo. The antenna covers the UWB frequency range of 3.4–11 GHz. Figure 3 depicts the parametric analysis of the proposed antenna, and Table 1 depicts the changes in design parameters in the evolution stages. The radius of the rings is fixed to 6.8 mm and 8.5 mm in the parametric design change 1 (PDC1). The ground plane length (d), width (b), and rectangular stub length (f) are fixed as 6 mm, 10.5 mm, and 3.6 mm, respectively. The length of the ground plane in PDC2 is changed to vary the impedance matching. The dimensions of b, d, and f are varied to achieve a UWB range (PDC3 and PDC4).

The antenna reflection coefficients curve is shown in Figure 4. The plot depicts −10 dB resonance at frequencies ranging from 3.4 to 11 GHz, covering the entire UWB spectrum. Figure 5 depicts the current distribution on the surface of the proposed unit cell. The surface current distribution is checked at 3.5 GHz, 6 GHz, 9 GHz, and 10.6 GHz frequencies. At 3.5 GHz, the current distribution is high in the centre of the antenna ring.

The surface current distribution reveals that the upper part of the circular ring contributes to the 6 GHz, whereas the current intensity is high over the outer ring and the

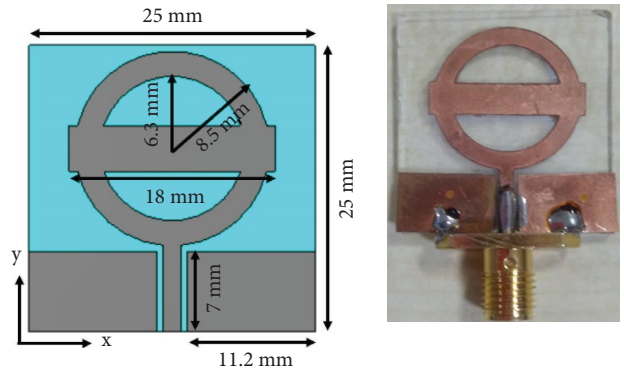

(a) (b)

Figure 1: Proposed antenna: (a) layout and (b) fabricated prototype.

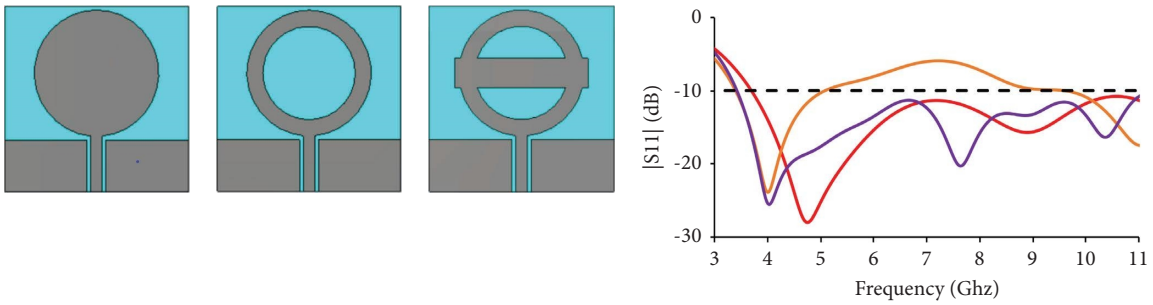

(a) (b) (c) (d)

Figure 2: (a) Evolution 1, (b) evolution 2, (c) evolution 3, and (d) reflection coefficients of the evolution stages.

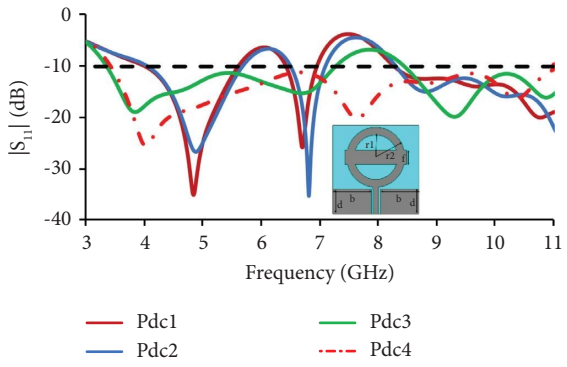

Figure 3: Reflection coefficient variations with the PDC.

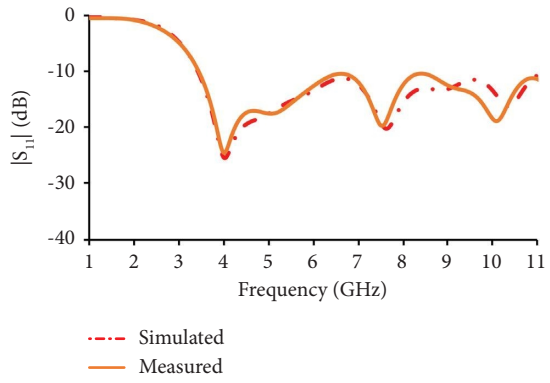

Figure 4: S_{11} of the proposed car logo-inspired antenna.

Table 1: Parameter dimensional changes (PDCs) in the evolution stages.

PDC	Parameter (mm)				
	r_1	r_2	f	b	d
1	6.8	8.5	3.6	10.5	6
2	6.8	8.5	3	10.5	6
3	6.8	8.5	3	11.2	7
4	6.3	8.5	4	11.2	7

ground plane at 9 GHz. The bottom part of the circular ring has the highest current intensity at 10.6 GHz.

2.1. Equivalent Circuit Design of the Proposed Antenna. The equivalent circuit is investigated in order to comprehend the physical mechanism of the antenna. The impedance characteristics and equivalent circuit of the unit cell antenna are shown in Figures 6(a) and 6(b), respectively. The

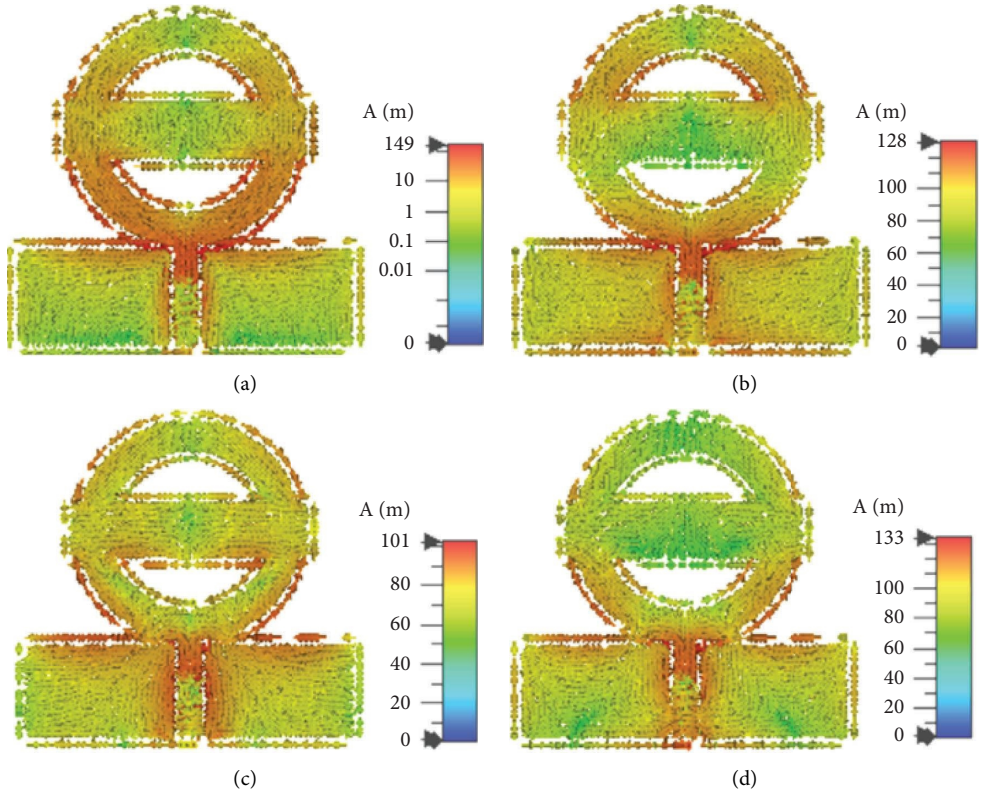

Figure 5: Surface current distribution at (a) 3.5 GHz, (b) 6 GHz, (c) 9 GHz, and (d) 10.6 GHz.

RLC values of the equivalent circuit are calculated using the following equations, where $\omega_0 = 2\pi f_0$ and $\omega_c = 2\pi f_c$ [30].

$$R = \left[\frac{2Z_0}{\sqrt{\left(1/|S_{11}|^2\right) - \left(2Z_0\left(C\omega_0 - \left(1/L\omega_0\right)\right)\right)^2 - 1}}\right],$$

$$L = \frac{Z_o}{2}\left(\frac{\omega_c}{\left(\omega_0^2 - \omega_c^2\right)}\right), \tag{1}$$

$$C = \frac{1}{\omega_0^2 L}.$$

The impedance characteristics are used to design the equivalent circuit. The three peak impedance points (4.02 GHz, 7.652 GHz, and 10.392 GHz) are chosen from the antenna's reflection coefficients to calculate the *RLC* values. When the impedance curves move from low to high, a series resonant circuit is formed, and when the curves move from high to low, a parallel resonant circuit is formed. Figure 6(c) compares the reflection coefficients calculated using the equivalent circuit to the simulated and measured values.

2.2. Orthogonal Quad-Port MIMO Antenna Design. The unit cell is developed into a four-port diversity antenna, shown in Figure 7, with orthogonal resonating elements. The orthogonal orientation of the antenna elements offers polarization diversity, with two polarization vectors (horizontal and vertical). MIMO/diversity in automotive antennas aids in signal reception from all directions. The perpendicular positioning of the unit cells has no effect on the reflection coefficient characteristics of the proposed MIMO antenna. Many techniques for increasing isolation have been reported in the literature, including EBG, metamaterial surfaces [31], FSS, neutralization line, parasitic elements, photonic bandgap (PBG), embedded periphery slot [32], and DGS. Though these decoupling methods have their own advantages, they can add complexity to the antenna design. The distance between each unit cell is kept as 6 mm, resulting in isolation greater than 15 dB without the use of any additional isolation structures. The size of the diversity antenna is 56 mm × 56 mm × 1.6 mm.

Figure 8 depicts the surface current distribution of the MIMO antenna. It demonstrates that the majority of the current exists in the feeding radiator (element-1) of the antenna known as the active zone. The neutral zone, which is the area around the nonfeeding radiators, has a lower current distribution. The surface current distribution is less, but not zero, in the neutral zone [33].

3. Results and Discussion

3.1. S_{ii} and S_{ij} Characteristics. The reflection coefficient characteristics and mutual coupling of the quad-port diversity antenna are investigated and plotted in Figures 9 and 10, respectively. The antenna exhibits stable performance across the resonating band. The S_{ij} characteristics are investigated in relation to antenna-1 and antenna-2, and

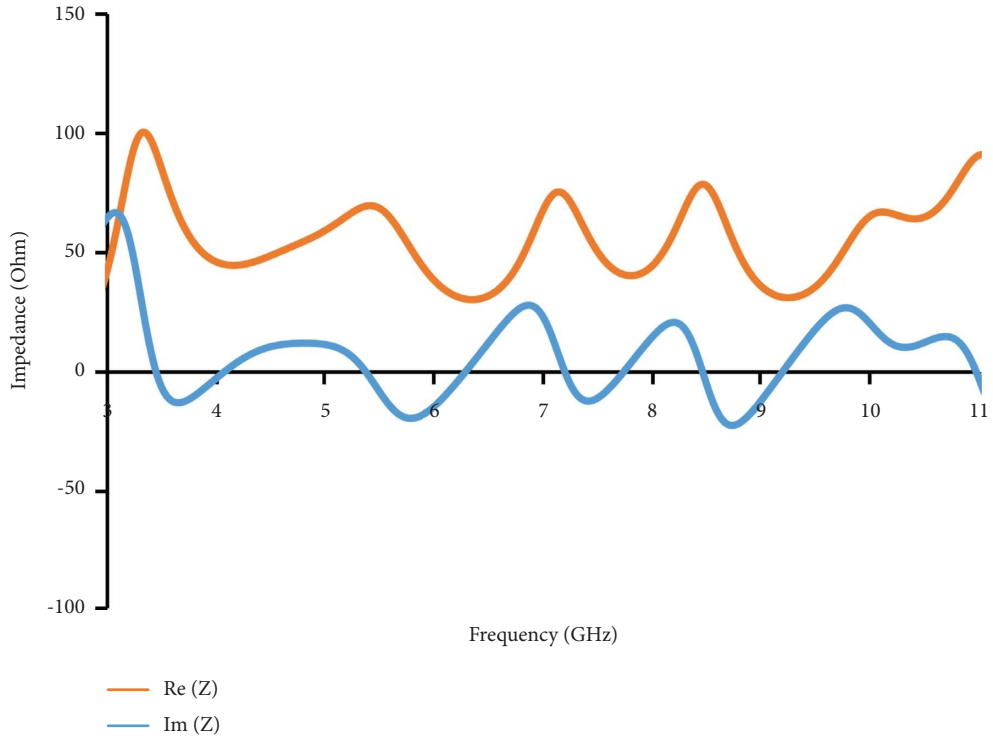

(a)

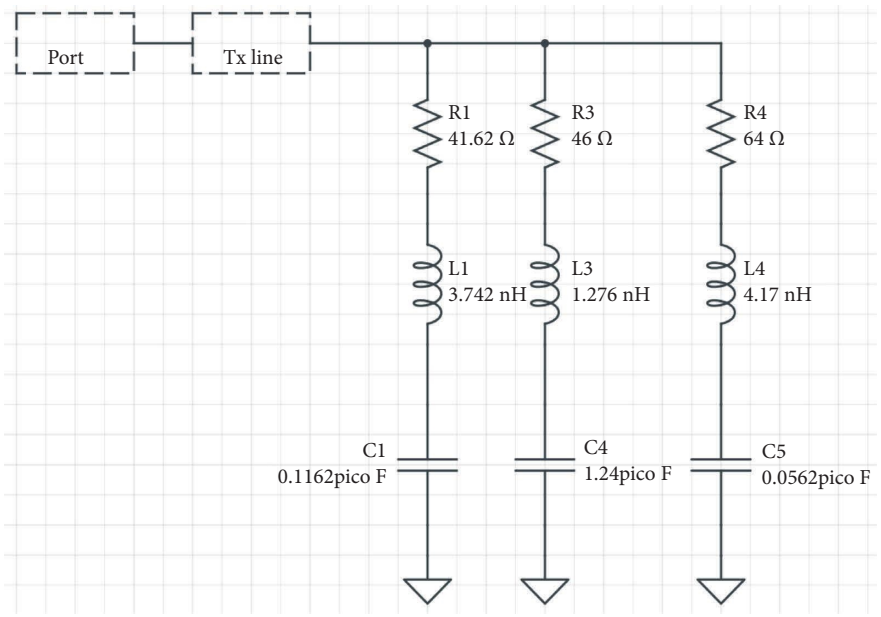

(b)

Figure 6: Continued.

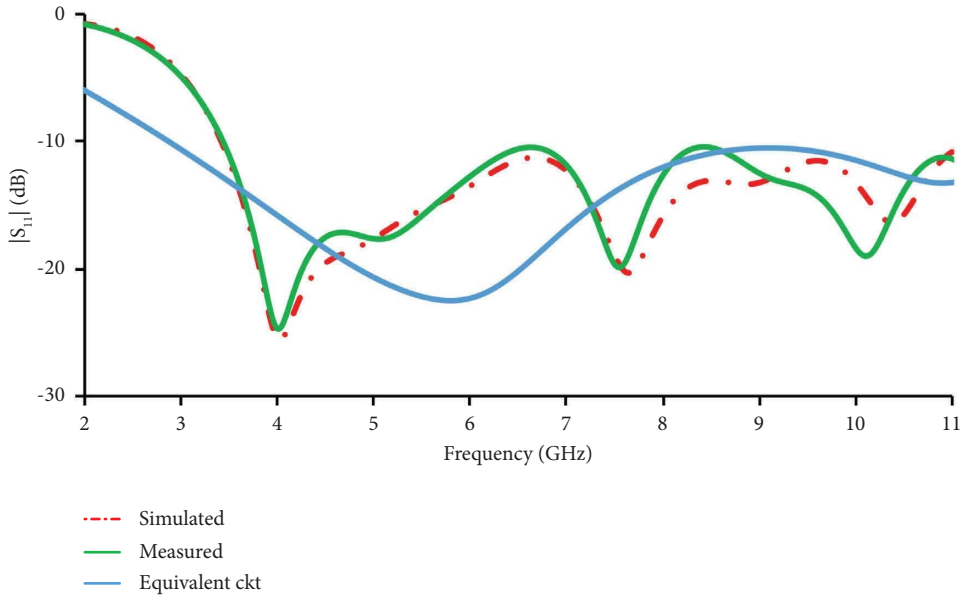

(c)

Figure 6: Proposed antenna: (a) impedance characteristics, (b) equivalent circuit, and (c) reflection coefficients.

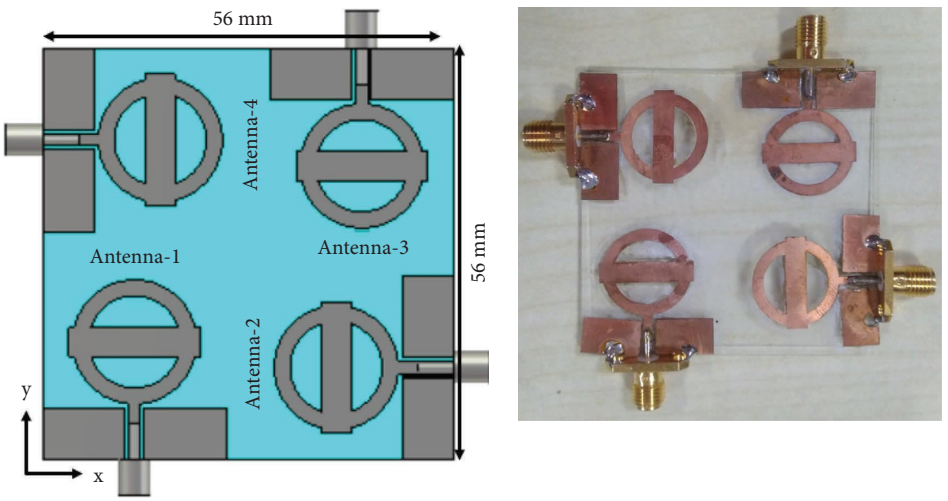

(a) (b)

Figure 7: Continued.

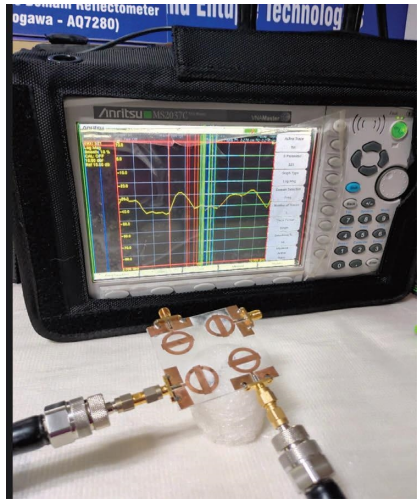

(c)

Figure 7: Orthogonal quad-port MIMO antenna: (a) layout, (b) prototype, and (c) VNA measurement setup.

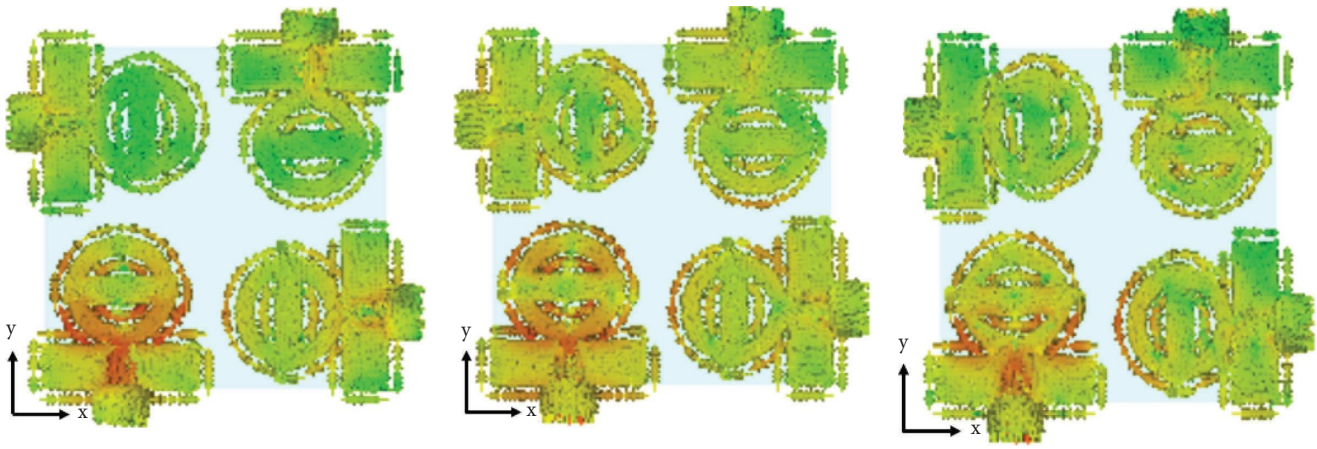

(a) (b) (c)

Figure 8: Surface current distribution of the MIMO antenna, when antenna element-1 is excited at (a) 3.5 GHz, (b) 6 GHz, and (c) 9 GHz.

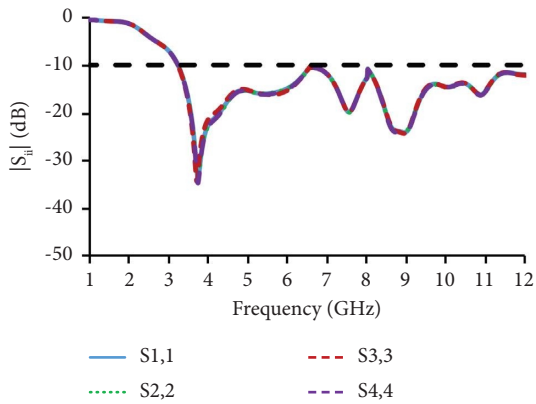

Figure 9: S_{ii} curves of the proposed antenna.

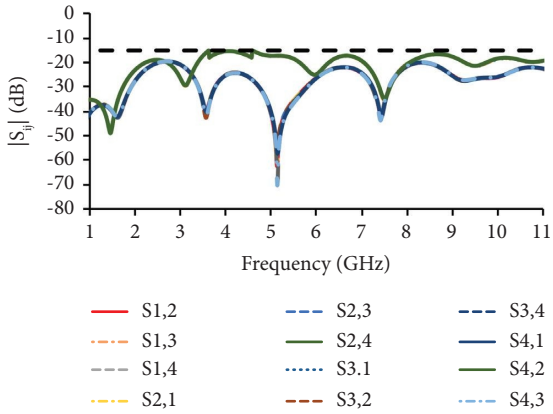

FIGURE 10: S_{ij} curves of the proposed antenna.

without using any additional mutual coupling reduction techniques, the isolation is greater than 15 dB.

3.2. Radiation Characteristics. The radiation pattern plots of the antenna are shown in Figure 11. The radiation pattern is shown for frequencies of 3.5, 6, 9, and 10.6 GHz. The copolarization and cross-polarization radiation patterns of the antenna are investigated. In copolarization, the polarization of both the transmitting and receiving antennas is the same, whereas in cross-polarization, the polarization of both antennas is different. The cross-polarization value is less than the copolarization value at all the frequencies. Figure 12 shows the gain and efficiency graphs. The maximum gain and efficiency of the proposed antenna are greater than 3.45 dBi and 97%, respectively.

3.3. Housing Effects of the Antenna

3.3.1. Reflection Coefficient and Far-Field Effect. The designed antenna is installed in the windshield of the car (shown in Figure 13(a)), and the reflection coefficient and far-field characteristics are investigated. Figures 13(b) and 13(c) present the antenna's reflection coefficients and far-field characteristics. The reflection coefficients illustrates that the antenna's performance is unaffected by its location in the vehicle. The far-field curves reveal that the antenna has near-omnidirectional properties and improved directivity.

3.3.2. Effect of Nearby Conductors on the Antenna. A metal plate with the antenna placed in two axes is examined to investigate the performance of the proposed antenna under the influence of other conductors, as shown in Figure 14. The metal plate has a size of 40 cm × 40 cm × 5 cm. The metal is a perfect conductor and serves as a large ground plane. The plate resembles the roof of the vehicle. The proposed antenna is positioned vertically (case-1) and horizontally (case-2) with respect to the metal plate. The distance between the antenna and the metal plate is kept as 1 cm. The S_{ii} properties of the antenna are investigated in the presence of a metal plate, shown in Figure 15, and the results are consistent.

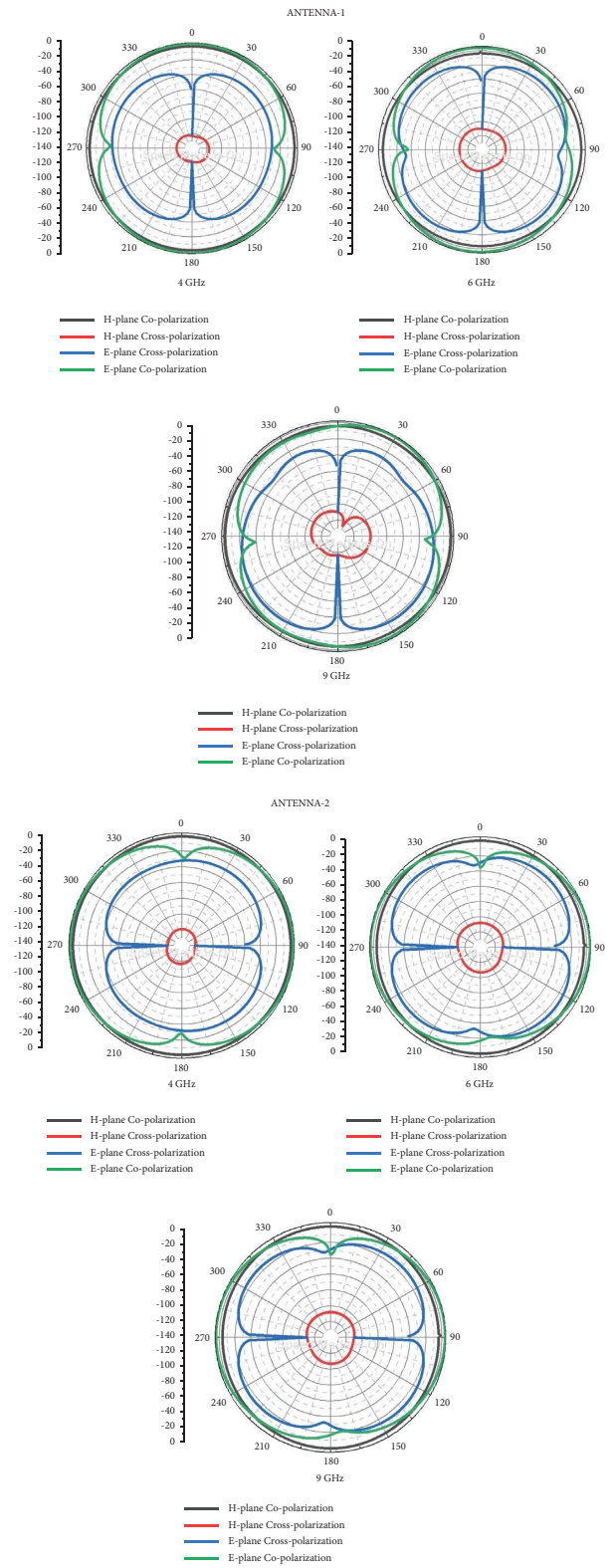

FIGURE 11: Radiation patterns of the developed MIMO antenna-1 and antenna-2.

3.4. Diversity Parameter Results. To understand the characteristics of the MIMO antenna, the diversity metrics are evaluated. The envelope correlation coefficient (ECC) describes how the antenna elements are related to one another.

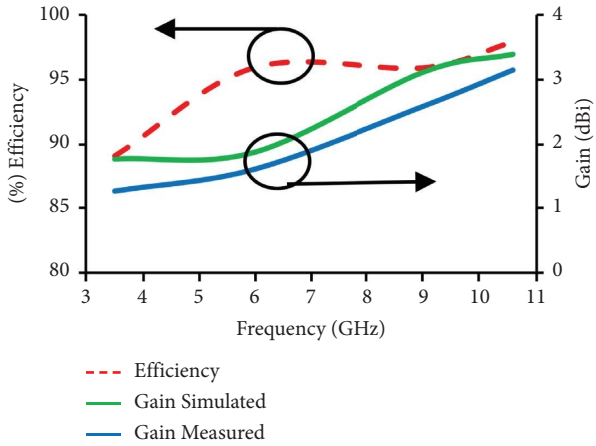

Figure 12: Gain and efficiency plots of the MIMO antenna.

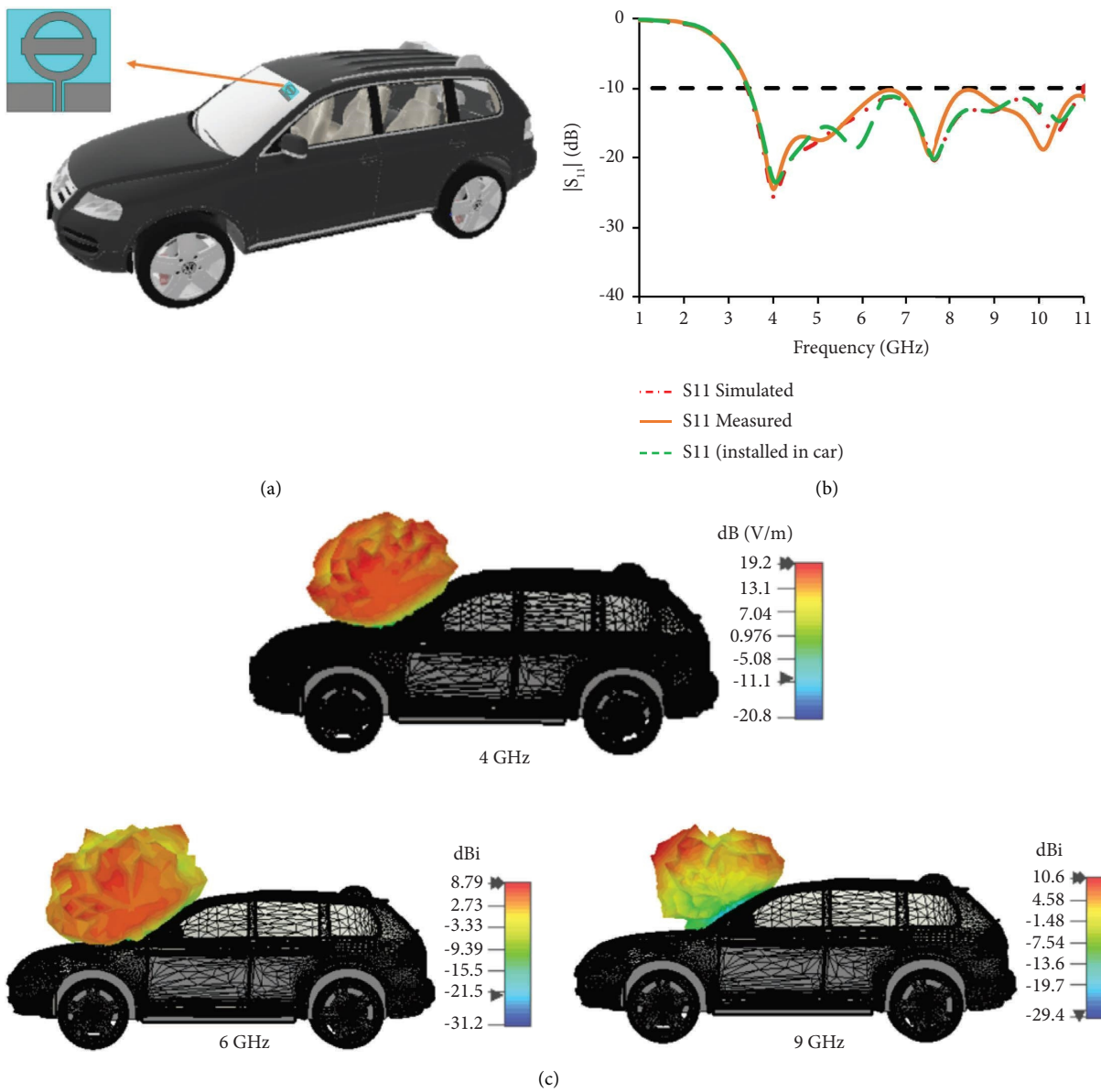

Figure 13: On-car performance of the proposed antenna: (a) placement, (b) reflection coefficients, and (c) far-field characteristics.

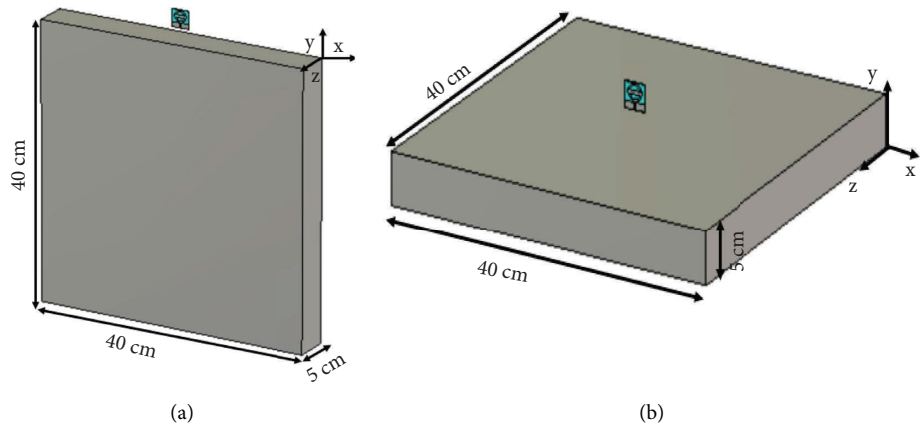

Figure 14: Housing effects: (a) case-1 and (b) case-2.

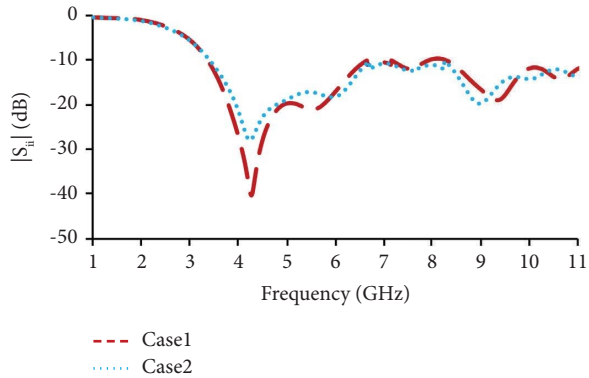

Figure 15: Reflection coefficients in the presence of a metal plate.

The ECC can be calculated using far-field and S-parameters [34]. The diversity performance plots are shown in Figures 16 and 17.

Other parameters such as diversity gain (DG), the total active reflection coefficient (TARC), and channel capacity loss (CCL) are calculated for antennas-1 and -2. The DG is also related to the ECC and is determined by the correlation among the antenna elements. TARC is an important parameter that relates to the reflection coefficient of the whole MIMO antenna [35]. The CCL is used to calculate transmission losses in the case of high data rate transmission [36].

Mean effective gain (MEG) is used to assess the ability of the antenna to accept electromagnetic power in a multipath environment. MEG is defined as the ratio of average power received by the antenna to the total powers received in the same environment if two isotropic antennas with vertical and horizontal polarization are used. Table 2 shows the MEG ratio of antenna-1 and antenna-2, which is close to unity for the desired frequencies.

Table 3 compares the proposed MIMO antenna with the previously reported antennas. The characteristics of the proposed work are as follows:

(1) Unlike other works reported in the literature [37–41], the proposed antenna is fabricated on a semitransparent substrate.

(2) The proposed antenna is investigated for the UWB, and the MIMO/diversity parameters are examined.

(3) The ECC, TARC, and CCL values of the proposed antenna are lower than those reported in the literature [37–41].

(4) Unlike previous works [38, 39, 41], the MIMO antenna provides dual polarization vectors.

(5) In comparison to the previous literature [37–41], the proposed MIMO antenna has a straightforward design. In [40], a rhombic-shaped radiator was presented with a partial ground plane, whereas the proposed antenna comprised of a circular ring with a rectangular stub radiator and a CPW feed. In [41], the antenna ground plane was provided at the back of the radiator, but in the designed MIMO antenna, the radiator and the ground plane are on the same side, making fabrication easier.

(6) Furthermore, no decoupling structure is used in the proposed design, contributing to its low complexity. The area covered by the radiating (metal) part over the substrate is reduced due to the minimal use of stubs and slots, resulting in a transparency of 52.26%. The proposed MIMO/diversity antenna is tested in the automobile windshield and shows satisfactory performance.

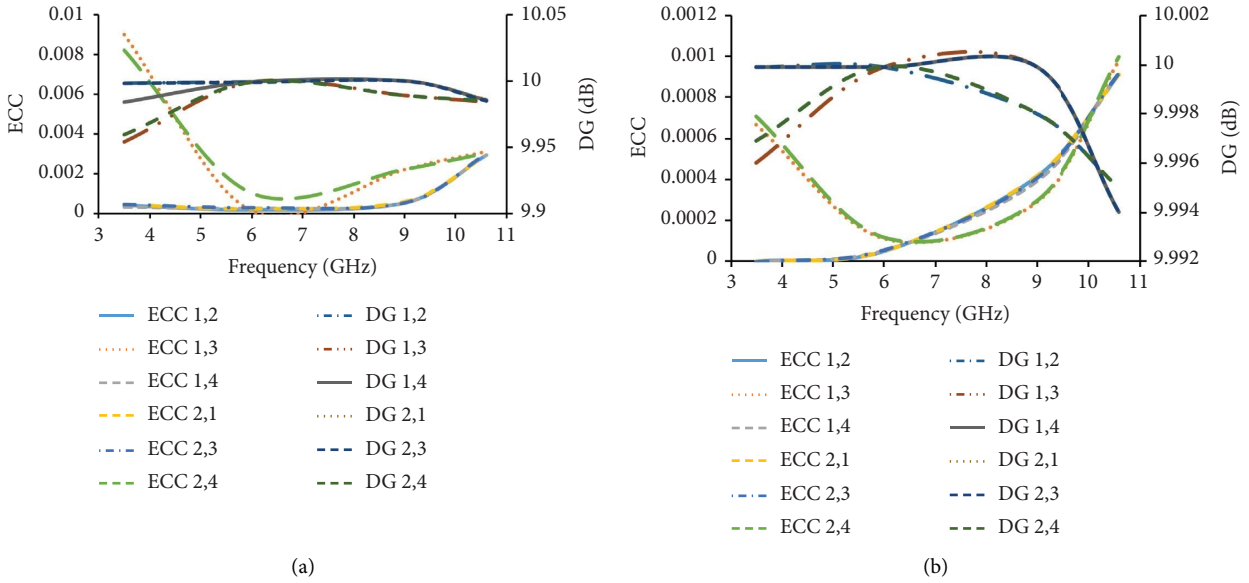

Figure 16: The ECC and DG of the antenna: (a) far-field and (b) s-parameters.

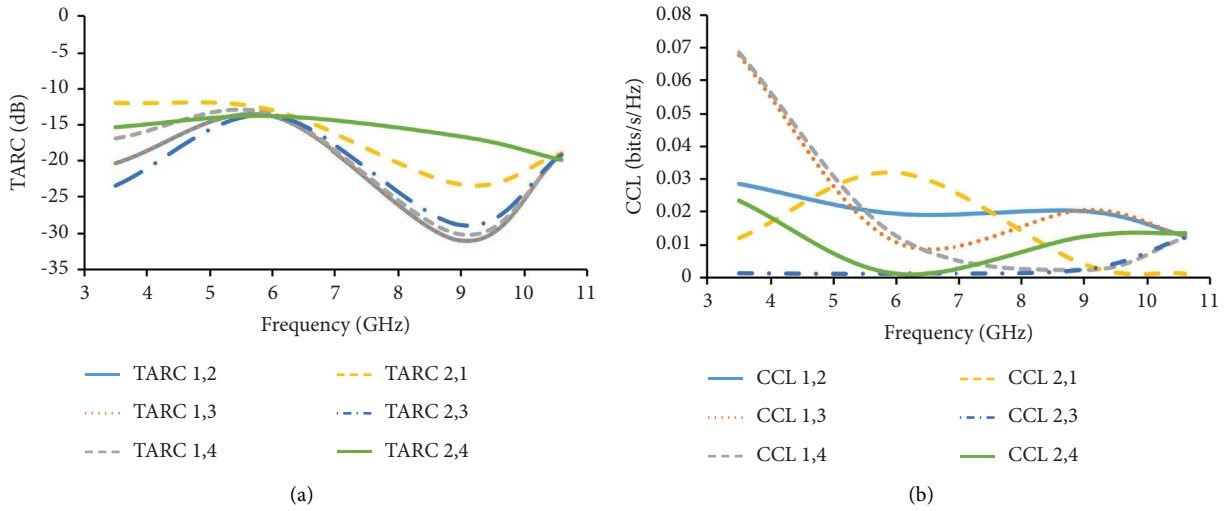

Figure 17: Performance of the MIMO antenna: (a) TARC and (b) CCL.

Table 2: MEG of the antenna-1 with respect to antenna-2.

Frequency (GHz)	Isotropic XPR = 0 dB MEG_1/MEG_2	Outdoor XPR = 1 dB MEG_1/MEG_2	Indoor XPR = 5 dB MEG_1/MEG_2
3.5	1	0.999	1
6	1	1	0.998
9	1	0.999	1
10.6	1	0.999	1

Table 3: Comparison of the proposed MIMO antenna with the previously reported antennas.

Ref	MIMO size (in terms of λ_0)	Substrate/Height (mm)	Operating frequency (GHz)	ECC	TARC (dB)	CCL (bits/s/Hz)	Transparency	Polarization	Design technique	Design complexity
[37]	0.2×0.2	FR-4/1.6	1.41–1.62, 2.4–2.462, 3.1–12.8	<0.4	<−10	<0.4	No	Dual	Stub, slot, DGS, and patch loading	High
[38]	0.372×0.112	Taconic/0.5	2.8–9.5	<0.4	—	—	No	Vertical	Sectoral slot and interlock	Moderate
[39]	0.245×0.261	Rogers RO4003C/0.2	2.45	<0.2	—	—	No	Vertical	Sectoral slot and circular slot	Moderate
[40]	0.672×0.672	FR-4/0.8	2.8–13.3	<0.05	—	—	No	Dual	Partial ground, CSRR, and rhombic radiator	Low
[41]	0.39×0.39	FR-4/1.6	3.72–3.82, 4.65–4.76, 6.16–6.46	<0.1	<−10	<0.8	No	Vertical	Rectangular monopole, slot, and full ground plane	Low
This work	0.636×0.636	Soda lime glass/ 1.1	3.4–11	<0.01	<−10	<0.07	Semitransparent	Dual	Circular ring and rectangular patch loading	Low

4. Conclusion

In this work, a semitransparent antenna is designed on a windshield substrate. The radiator of the antenna is similar to the "NISSAN automobile-like" logo, and its implementation does not affect the aesthetic appearance of the vehicle. The antenna has an impedance bandwidth of −10 dB over a frequency range of 3.4–11 GHz. The unit cells are combined to form a four-port MIMO antenna with more than 15 dB of interelement isolation. The diversity performance metrics of the MIMO antenna show ECC < 0.01, DG > 9.98 dB, TARC < −10 dB, CCL < 0.07 bits/s/Hz, and MEG ratio close to unity, which meets the practical limits. The reliability of the antenna is tested on a vehicle, and it performs satisfactorily. The antenna prototype can be installed in the windshield, side, front, or rear mirror. In the future, the antenna could be developed on a completely transparent substrate, with transparent thin films as radiators and ground planes.

Data Availability

The data used to support the findings of this study are available from the corresponding author upon request.

Conflicts of Interest

The authors declare that they have no conflicts of interest.

References

[1] H. Honggang, L. Jiayu, H. Daili, and L. Wei, "Design of hexagon microstrip antenna for vehicle-to-vehicle communication," *The Journal of China Universities of Posts and Telecommunications*, vol. 23, no. 4, pp. 69–76, 2016.

[2] B. Rammyaa and K. S. Vishvaksenan, "CPW fed metamaterial loaded dual-band roof-top antenna for vehicular communications," *International Journal of RF and Microwave Computer-Aided Engineering*, vol. 31, no. 8, 2021.

[3] S. Ibrahim, A. M. Yacoub, and D. N. Aloi, "A 3-A 3-Dimensional Multiband Antenna for Vehicular 5G Sub-6 GHz/GNSS/V2X Applicationsimensional multiband antenna for vehicular 5G sub-6 GHz/GNSS/V2X applications," *International Journal of Antennas and Propagation*, vol. 2022, Article ID 5609110, 13 pages, 2022.

[4] Q. Wu, Y. Zhou, and S. Guo, "An L-An L-Sleeve L-Monopole Antenna Fitting a Shark-Fin Module for Vehicular LTE, WLAN, and Car-to-Car Communicationsleeve L-monopole antenna fitting a shark-fin module for vehicular LTE, WLAN, and car-to-car communications," *IEEE Transactions on Vehicular Technology*, vol. 67, no. 8, pp. 7170–7180, 2018.

[5] M. A. Chung and C. W. Yang, "A A miniaturized planar monopole antenna based on a coupling structure for compact mobile internet of things (IoT) and electric vehicles (EVs) device applications in 5G, LTE, WLAN, WiMAX, sirius/XM radio, V2X, and dsrc wireless systemsiniaturized planar monopole antenna based on a coupling structure for compact mobile internet of things (IoT) and electric vehicles (EVs) device applications in 5G, LTE, WLAN, WiMAX, sirius/XM radio, V2X, and dsrc wireless systems," *International Journal of Antennas and Propagation*, vol. 2021, Article ID 7535382, 12 pages, 2021.

[6] L. Wang, J. Yu, T. Xie, and K. Bi, "A A novel multiband fractal antenna for wireless applicationovel multiband fractal antenna for wireless application," *International Journal of Antennas and Propagation*, vol. 2021, Article ID 9926753, 9 pages, 2021.

[7] S. Kingsly, D. Thangarasu, M. Kanagasabai et al., "Tunable band-notched high selective UWB filtering monopole antenna," *IEEE Transactions on Antennas and Propagation*, vol. 67, no. 8, pp. 5658–5661, 2019.

[8] R. G. S. Alsultan and G. Ögücü Yetkin, "Mutual coupling reduction of E-shaped MIMO antenna with matrix of C-shaped resonators," *International Journal of Antennas and Propagation*, vol. 2018, Article ID 4814176, 13 pages, 2018.

[9] A. Christina Josephine Malathi and D. Thiripurasundari, "Review on review on isolation techniques in MIMO antenna systemssolation techniques in MIMO antenna systems," *Indian Journal of Science and Technology*, vol. 9, no. 35, 2016.

[10] V. S. D. Rekha, P. Pardhasaradhi, B. T. P. Madhav, and Y. U. Devi, "Dual dual band notched orthogonal 4-element MIMO antenna with isolation for UWB aand notched orthogonal 4-element MIMO antenna with isolation for UWB applications," *IEEE Access*, vol. 8, pp. 145871–145880, 2020.

[11] A. Q. A. Kumar, A. Q. Ansari, B. K. Kanaujia, J. Kishor, and S. Kumar, "An ultra-compact two-port UWB-MIMO antenna with dual band-notched characteristics," *AEU - International Journal of Electronics and Communications*, vol. 114, Article ID 152997, 2020.

[12] L. Wang, Z. Du, H. Yang et al., "Compact UWB MIMO compact UWB MIMO antenna with high isolation using fence-type decoupling structurentenna with high isolation using fence-type decoupling structure," *IEEE Antennas and Wireless Propagation Letters*, vol. 18, no. 8, pp. 1641–1645, 2019.

[13] P. Kumar, S. Urooj, and F. Alrowais, "Design and implementation of quad-port MIMO antenna with dual-band elimination characteristics for ultra-wideband applications," *Applied Sciences*, vol. 10, no. 5, p. 1715, 2020.

[14] D. Gopi, A. Kumari, A. K. Talamarla, A. Joka, and N. M. S. Krishna, "CPW-fed conformal ESP antenna for vehicular applications," *Journal of Physics: Conference Series*, vol. 1706, 2020.

[15] J. I. Trujillo Flores, R. Torrealba Melendez, J. M. Munoz Pacheco et al., "CPW-fed transparent antenna for vehicle communications," *Applied Sciences*, vol. 10, no. 17, p. 6001, 2020.

[16] P. Kumar, S. Urooj, and F. Alrowais, "Design of quad-port MIMO/diversity antenna with triple-band elimination characteristics for super-wideband applications," *Sensors*, vol. 20, no. 3, p. 624, 2020.

[17] S. K. Palaniswamy, M. Kanagasabai, S. Arun Kumar et al., "Super wideband printed monopole antenna for ultra-wideband applications," *International Journal of Microwave and Wireless Technologies*, vol. 9, no. 1, pp. 133–141, 2017.

[18] A. Rahman and A. Watanabe, "Flexible and flexible and semi-transparent antenna for ISM band fabricated by direct laser writingemi-transparent antenna for ISM band fabricated by direct laser writing," *Journal of Photopolymer Science and Technology*, vol. 34, no. 2, pp. 149–153, 2021.

[19] A. Desai, T. Upadhyaya, J. Patel, R. Patel, and M. Palandoken, "Flexible CPW fed transparent antenna for WLAN and sub-6 GHz 5G applications," *Microwave and Optical Technology Letters*, vol. 62, no. 5, pp. 2090–2103, 2020.

[20] A. Desai, T. Upadhyaya, and R. Patel, "Compact wideband transparent antenna for 5G communication systems,"

Microwave and Optical Technology Letters, vol. 61, no. 3, pp. 781–786, 2019.

[21] A. Babu, B. T. P. Madhav, B. Vineel, G. Chandhini, C. Amrutha, and M. C. Rao, "Design and analysis of a circularly polarized flexible, compact and transparent antenna for vehicular communication applications," *Journal of Physics: Conference Series*, vol. 1804, 2021.

[22] D. Jang, N. K. Kong, and H. Choo, "Design of an design of an on-glass 5G monopole antenna for a vehicle window glassn-glass 5G monopole antenna for a vehicle window glass," *IEEE Access*, vol. 9, pp. 152749–152755, 2021.

[23] M. C. Lim, S. K. A. Rahim, M. R. Hamid, P. J. Soh, and A. Eteng, "Semi-transparent frequency reconfigurable antenna with DGS," *Microwave and Optical Technology Letters*, vol. 60, no. 1, pp. 6–13, 2018.

[24] S. Bandi, D. K. Nayak, B. T. P. Madhav, and A. Tirunagari, "Transparent circular monopole antenna for automotive communication," *Applied Computational Electromagnetics Society Journal*, vol. 34, pp. 704–708, 2019.

[25] T. Ali and R. C. Biradar, "A miniaturized volkswagen logo UWB antenna with slotted ground structure and metamaterial for GPS, WIMAX and WLAN applications," *Progress In Electromagnetics Research C C*, vol. 72, pp. 29–41, 2017.

[26] A. Ameelia Roseline, K. A. Malathi, Roseline, and K. Malathi, "Compact dual-band patch antenna using spiral shaped electromagnetic bandgap structures for high speed wireless networks," *AEU - International Journal of Electronics and Communications*, vol. 66, no. 12, pp. 963–968, 2012.

[27] K. Li, C. H. Cheng, T. Matsui, and M. Izutsu, "Coplanar patch antennas: principle, simulation and experiment," *IEEE Antennas and Propagation Society*, vol. 3, pp. 402–405, 2001.

[28] J. Liang, L. Guo, C. C. Chiau, and X. Chen, "CPW-fed circular disc monopole antenna for UWB applications," in *Proceedings of the 2005 IEEE International Workshop on Antenna Technology: Small Antennas and Novel Metamaterials*, pp. 505–508, Singapore, March 2005.

[29] B. R. Rao and P. V. Sridevi, "Design of finite ground coplanar waveguide (FGCPW) fed strip monopole antenna for WLAN applications," in *Proceedings of the International Conference on Communication and Signal Processing*, pp. 607–611, Melmaruvathur, India, April 2013.

[30] R. Sanyal, P. P. Sarkar, and S. Sarkar, "Octagonal nut shaped monopole UWB antenna with sextuple band notched characteristics," *AEU - International Journal of Electronics and Communications*, vol. 110, Article ID 152833, 2019.

[31] N. Kumar and U. K. Kommuri, "MIMO antenna H-plane isolation enhancement using UC-EBG structure and metal line strip for WLAN applications," *Radioengineering*, vol. 27, no. 2, pp. 399–406, 2019.

[32] M. Alibakhshikenari, B. S. Virdee, P. Shukla et al., "Antenna mutual coupling suppression over wideband using embedded periphery slot for antenna arrays," *Electronics*, vol. 7, no. 9, p. 198, 2018.

[33] V. Satam, S. Nema, and S. S. Thakur, "Spanner shape monopole MIMO antenna with high gain for UWB applications," *Lecture Notes on Data Engineering and Communications Technologies*, vol. 19, pp. 129–138, 2018.

[34] S. Basir, K. S. Alimgeer, S. A Ghauri, M. Maqsood, M. Sarfraz, and M. Y. Ali, "MIMO MIMO Antenna with Notches for UWB System (MANUS)ntenna with notches for UWB systems (MANUS)," *International Journal of Antennas and Propagation*, vol. 2022, Article ID 4870661, 8 pages, 2022.

[35] D. Subitha, S. Velmurugan, M. V. Lakshmi, P. Poonkuzhali, T. Yuvaraja, and S. Alemayehu, "Development of development of rogers RT/duroid 5880 substrate-based MIMO antenna array for automotive radar applicationsogers RT/duroid 5880 substrate-based MIMO antenna array for automotive radar applications," *Advances in Materials Science and Engineering*, vol. 2022, Article ID 4319549, 11 pages, 2022.

[36] G. Thennarasi, S. K. Palaniswamy, M. Kanagasabai, S. Kumar, T. R. Rao, and M. G. N. Alsath, "Conformal quad-port UWB MIMO antenna for body-worn applications," *International Journal of Antennas and Propagation*, vol. 2021, Article ID 9409785, 13 pages, 2021.

[37] L. Kannappan, S. K. Palaniswamy, L. Wang et al., "Quad-port multiservice diversity antenna for automotive applications," *Sensors*, vol. 21, no. 24, p. 8238, 2021.

[38] M. Saravanan, R. Kalidoss, B. Partibane, and K. S. Vishvaksenan, "Design of an interlocked four-port MIMO antenna for UWB automotive communications," *International Journal of Microwave and Wireless Technologies*, vol. 14, no. 2, pp. 239–246, 2022.

[39] M. Ramesh and C. Geetha Priya, "Miniaturized four port MIMO antenna for automotive communications," *Analog Integrated Circuits and Signal Processing*, vol. 111, no. 1, pp. 25–33, 2022.

[40] S. Kumar, G. H. Lee, D. H. Kim, W. Mohyuddin, H. C. Choi, and K. W. Kim, "Multiple-input-multiple-output/diversity antenna with dual band-notched characteristics for ultra-wideband applications," *Microwave and Optical Technology Letters*, vol. 62, no. 1, pp. 336–345, 2020.

[41] R. Krishnamoorthy, A. Desai, R. Patel, and A. Grover, "4 Element compact triple band MIMO antenna for sub-6 GHz 5G wireless applications," *Wireless Networks*, vol. 27, no. 6, pp. 3747–3759, 2021.